

## **Voltammetric Analysis of Thiamethoxam Based on Inexpensive Thick-Walled Moso Bamboo Biochar Nanocomposites**

Shangxing Chen<sup>1,†</sup>, Linjian Li<sup>2,†</sup>, Yangping Wen<sup>2,3</sup>, Guangyao Yang<sup>4</sup>, Guangbin Liu<sup>2,\*</sup>, Yufu Yi<sup>1,2</sup>, Qingyin Shang<sup>3</sup>, Xiuxia Yang<sup>3,\*</sup>, Shuo Cai<sup>2,5</sup>

<sup>1</sup> Collaborative Innovation Center of Jiangxi Typical Trees Cultivation and Utilization, Jiangxi Agricultural University, Nanchang 330045, China

<sup>2</sup> Institute of Functional Materials and Agricultural Applied Chemistry, Jiangxi Agricultural University, Nanchang 330045, China

<sup>3</sup> Key Laboratory of Crop Physiology, Ecology and Genetic Breeding, Ministry of Education, Jiangxi Agricultural University, Nanchang 330045, China

<sup>4</sup> Jiangxi Provincial Key Laboratory for Bamboo Germplasm Resources and Utilization, Jiangxi Agricultural University, Nanchang 330045, China

<sup>5</sup> Jiangxi Key Laboratory of Agricultural Efficient Water-Saving and Non-Point Source Pollution Preventing, Jiangxi Central Station of Irrigation Experiment, Nanchang 330201, China

\*E-mail: [lgb267@126.com](mailto:lgb267@126.com), [yangxiuxia11@163.com](mailto:yangxiuxia11@163.com)

<sup>†</sup>These authors contributed equally to the article.

*Received:* 9 August 2019 / *Accepted:* 22 September 2019 / *Published:* 29 October 2019

---

A simple and cheap thick-walled Moso biochar (BC) was selected and combined with carbonate minerals dolomite (DM) to construct a voltammetric sensing platform for application in stripping analysis of thiamethoxam in agricultural and environmental samples. The BC based on thick-walled Moso was prepared by pyrolyzing biomass wastes in limited oxygen atmosphere at temperatures of 600 °C for 2 h, and the BC-DM nanocomposite was obtained through milling and sieving, then liquid-phase ultrasonic assistance by dispersing grinded DM and moso bamboo BC into ultra-pure water. The morphology and structure of the BC-DM nanocomposite were characterized by FT-IR, XRD, and SEM-EDX. Under optimal conditions, the BC-DM modified electrode showed high sensitivity and good stripping voltammetric response towards thiamethoxam in a linear range from 0.5 to 35 µg mL<sup>-1</sup> with a limit of detection (LOD) of 0.22 µg mL<sup>-1</sup>. The prepared nanocomposite sensor was employed for the determination of thiamethoxam in different real samples with acceptable recoveries. Thick-walled moso as biochar with post-modification provides a new promising platform for potential applications in electrochemistry.

---

**Keywords:** Bamboo; biochar; dolomite; thiamethoxam; sensor; electrochemistry.

## 1. INTRODUCTION

Thiamethoxam, also called 3-(2-chloro-1,3-thiazol-5-ylmethyl)-5-methyl-1,3,5-oxadiazinane-4-ylidene(nitro) amine, is a new type of contact insecticides, which can effectively inhibit aphids, thrips, leafhoppers and mealworms [1, 2]. Thiamethoxam has been widely used as plant protecting agent in many countries, but its residue can cause irreversible damage to the environment. Therefore, it is necessary to establish a rapid and sensitive way to detect the residue of thiamethoxam in the environment and agricultural products. Various methods like high-performance liquid chromatography with diode-array [3], mass-spectrometry [4, 5], enzyme-linked immunosorbent assay [6], and differential pulse polarography [7] have been developed to detect thiamethoxam with satisfactory accuracy in practical application. However, shortcomings still exist in these methods, including high testing costs, expensive apparatuses, complicated samples pretreatment and time-consuming operating processes. Thus, electroanalysis, especially chemically modified electrodes (CME), has become a powerful tool to detect and analyze the residual pollutant of thiamethoxam in agricultural and environmental samples due to their high electrocatalytic activity and large surface area, rapid response, low reagent consumption and simple operation. Recently, multiple nanomaterials, as highly-sensitive nanocomposite for CME, have attracted tremendous interests in exploring/exploiting the potential application of efficient electrochemical sensors.

Biochar (BC), an emerging carbon-rich solid material, is commonly made by pyrolyzing biomass wastes under anoxic atmosphere at a certain temperature. Generally, BC was employed as active absorption materials in agriculture and environments to remove organics [8-11], heavy metal [12-14], dyes [15-17] and purifying water quality [18,19] owing to its extraordinary porous properties. With more in-depth research, BC has been applied as new sustainable electrode materials in electrochemical applications including energy storage and conversion [20], sensing analysis [21], and so on [22,23]. These progress not only promote the new method of post-modification for raw BC, but also facilitate several ways to improve the electrochemical properties of BC [24-26]. In our previous work, we have developed a pitch pine BC with water-processability and investigated its potential application in electrochemical sensing of cadmium ions [27]. Subsequently, we prepared a micro/nano BC with satisfactory water-dispersibility and further explored their potential applications in electrochemical sensors, fertilizers, biofuels, and heavy metal adsorbents [28]. Besides, we found that natural mineral materials like palygorskite [29,30], halloysite [31], and montmorillonite [32] combined with carbon nanomaterials will amplify electrochemical signal and increase specific surface area.

Bamboo is one of the most significant non-timber forest products in the world, about 2.5 billion people depend economically on bamboo, and over 2.5 billion US dollars acquire from international trade in bamboo amounts per year. Bamboo has great potential as a biomass material and bio-energy resource of the future due to its advantages such as fast growth and high strength. At present, the area of bamboo is about five million hectares in China, of which moso bamboo accounts for 60% [33]. Bamboo can be carbonized into a hierarchical porous carbonaceous structure, which makes bamboo BC with a highly ordered structure and possesses large surface area, high conductivity, well connectivity as a high-performance supercapacitor electrode material

via post-modification of polyaniline. Bamboo BC with microporous structure was also used for lithium-sulfur battery [34].

Inspired by this progress, we developed a BC based on thick-walled Moso bamboo, which was carbonized at 600 °C under oxygen-limited conditions and processed by crushing and grinding [35], after that BC-DM nanocomposite was prepared through liquid-phase ultrasonic assistance by dispersing the grinded dolomite (DM) and moso bamboo BC in ultra-pure water. Then the water-dispersible BC-DM nanocomposite was characterized by FT-IR, XRD, SEM-EDX, and successfully applied as a new electrode modified material for the detection of thiamethoxam using differential pulse stripping voltammetry (DPSV).

## 2. MATERIALS AND METHODS

### 2.1 Chemicals and reagents

Thick-walled Moso (*Phyllostachys pubescens* cv *Pachyloen*) is one of the new species of moso bamboo, which was bred and studied by Jiangxi Agricultural University and Forestry Research Institution of Yifeng County. DM was provided by Red Soil Institution of Jiangxi province. Britton-Robinson (B-R) buffer solution was prepared from acetic acid, boric acid and phosphoric acid solutions, while acetic acid was obtained from Tianjin Yongda Chemical Reagent Co., Ltd, boric acid was obtained from Tianjing Damao chemical reagent co., Ltd and phosphoric acid was bought from Xilong Chemical co., Ltd. Nafion D-521 dispersion (5% w/w in water and 1-propanol,  $\geq 0.92$  meq g<sup>-1</sup> exchange capacity). Thiamethoxam was obtained from Aladdin (Aladdin biotechnology co., LTD, Shanghai, China) and dissolved with double distilled water. All solutions were prepared by double distilled water and all reagents were analytical grade and used as received.

### 2.2 Instrumentation

The electrochemical measurement was performed on CHI660E Electrochemical workstation with a conventional three-electrode system (Chenhua Instruments Co., Shanghai, China). The working electrode was prepared as indicated below, platinum wire as counter electrode and the saturated calomel electrode (SCE) as the reference electrode. The CT-6023 portable pH meter was used to record the pH (Shanghai Jingmi Instrument, China). The water-processable BC was acquired using ultrasound instrument (Xingzhi Bio-tech. Ltd. Co., Ningbo, China). SEM-EDX were used scanning electron microscopy (SEM, Quanta F250, FEI Quanta, FEI, USA) and Energy Dispersive X-Ray Spectroscopy (EDX, GENESIS, EDAX, USA). The Magna-IR 750 fourier transform infrared spectrometer was employ for collected FTIR spectra (Thermo Nicolet Company, United States). The D8 X-ray diffractometer was applied for measured X-ray diffraction (XRD) (Bruker Ltd., German). BC was pulverized by a high-speed universal pulverizer (FW-400A, Linda Machinery Co., LTD. Zhejiang).

### 2.3 Preparation of Moso bamboo BC

The dusts on the surface of thick-walled Moso was completely cleaned when sampling. Then bamboo was sawed into pieces, the sawdust was collected and washed with double distilled water to remove impurities. Then it was over-dried for 5 h under the temperature of 85 °C to get rid of excess water in an air-blower-driven drying oven. The dried sawdust was passed through a 1.2-mm sieve after ground by a pulverizer for 15 min. Finally, the dried sawdust was placed in a tailor-made sealed stainless-steel jar and treated with heating to 600 °C for 2 h under set a limit of oxygen conditions until no excessive smoke escaped from the muffle furnace. The BC cools to room temperature. Finally, all BC is stored under condition with desiccator.

### 2.4 Preparation of BC-DM nanocomposite

BC was mixed with DM at the mass ratio of 2:1 and treated by milling through a variable frequency planet-type grinding mill, 2 hours later, the mixture with micro/nano-powders were sieved by an stainless steel screen (38.5  $\mu\text{m}$  mesh). Finally, a 21 mg mixture was added into 10 mL double distilled water and ultrasound for 30 min to form a suspension with both 1.4  $\text{mg mL}^{-1}$  BC and 0.7  $\text{mg mL}^{-1}$  DM. In addition, 0.5% Nafion (Nafion can enhance electrode stability [36], the immobilization of biomacromolecules [37], electrochemical catalytic responses [38], cation exchange [28], and so on) was used as an adhesive to stabilize a mixture of BC and DM on the surface of GCE.

### 2.5 Preparation of modified electrode

Prior to the modification, the bare GC electrode was polished on the chamois leather with 0.05  $\mu\text{m}$   $\text{Al}_2\text{O}_3$  slurry for 5 min. Then sonicated in doubly distilled water, anhydrous ethanol and doubly distilled water for 5 min in sequence, and it was dried under the infrared lamp. Finally, the GCE was placed in 0.5M  $\text{K}_3[\text{Fe}(\text{CN})_6]$  solution to check whether it is cleaned. The GCE was used when peak to peak separation between oxidation peak and reduction peak was less than 80 mV. A 5  $\mu\text{L}$  mixture of BC and DM containing Nafion was droplet coating on the surface of GCE after ultrasonic for 30 min, the nanocomposite modified electrode was prepared after the solvent evaporated in infrared dryer.

### 2.6 Preparation of real samples

Eight real samples including spinach, rice, pear, red soil, tap water, farmland water, river water, and lake water were prepared for simulating practical application. The spinach, rice and pear were got from local supermarket. Spinach and pear were carefully washed with double distilled water and cut into small pieces then dried in air. Rice was pulverized by a universal high-speed smashing machine for fifteen minutes. All of them (spinach, rice, pear) were in a mass ratio with double distilled water/samples of 10/1 put into juice. The red soil was provided by Jiangxi Institute of Red Soil and added double distilled water distilled water/samples of 10/1. tap water was obtained from the campus

in Jiangxi Agriculture University, farmland water, river water, and lake water were obtained from Jiangxi Central Station of Irrigation Experiment. All eight samples were centrifuged at 11000 rpm for 10 min at room temperature, the pH value of all real samples mentioned-above was adjusted to 5.0 with B-R buffer. Finally, all prepared sample solutions were employed as electrolytes and 5 ml thiamethoxam with different content in the real sample was conducted under optimal conditions using DPSV.

### 2.7 Electrochemical measurements

DPSV was performed in a 5 mL cell containing 0.1 M B-R buffer solutions on a CHI660E electrochemical workstation system. All experimental measurements were taken in the potential range from -0.7 to -0.3 V at the following parameters: preconcentration time is 300 s, deposition potential is -1.5 V and deposition time is 90 s. Prior to next measurement, the electrode surface was renewed to remove thiamethoxam. Thiamethoxam was added to cell by standard addition method and each experience repeated three times. All experiments were under the optimized conditions at room temperature.

## 3. RESULTS AND DISCUSSION

### 3.1 Morphology analysis

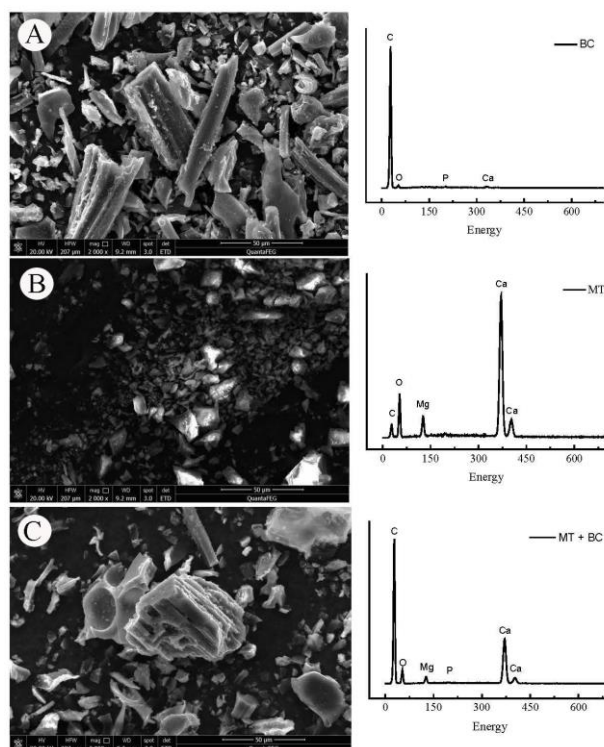


**Figure 1.** SEM images (left) and corresponding EDX spectra (right) of the three samples: (A) BC, 2000X; (B) DM, 2000X; and (C) BC-DM composite, 2000X. The EDX spectra were obtained at the same location as shown in the SEM images.

Fig. 1 shows SEM images and corresponding EDX elemental analysis spectra of three samples. Obviously, a block or strip with a distinctive honeycomb structure can be seen in Fig. 1A, which is highly heterogeneous with a large degree of macro-porosity in the 1 to 50  $\mu\text{m}$ , and large amounts of C and less amount of Ca, O and P elements was also found in relative EDX spectra. DM powder is irregularly shaped particles and non-agglomerated, in Fig. 1B, the small particles with size between 5 and 10  $\mu\text{m}$  can be seen. These ores mainly consist of  $\text{CaMg}(\text{CO}_3)_2$ , with relatively high concentrations of Ca, Mg, C, and O elements in there typical samples, which is consistent with EDX spectra in Fig. 1B. The surface of the BC is readily seen evenly distributed across the DM powder (Fig. 1C). The surface of composite material kept the original morphological structure. DM fragments exhibit edges of cleavage planes that are no longer straight and smooth but are rounded and rough due to dissolution. As evidenced shown in EDX spectra at the same location, a higher spectrum peak of magnesium and calcium relative to the BC can be seen.

### 3.2 Structural analysis

The FTIR spectrum peaks shows at Fig. 2, clearly, it was composed of multifarious bands. A couple of bands were proved correlation with oxygen-containing groups. The FTIR spectra of BC were characterized by four principal bands at the following wavelengths: The bands at  $3436\text{ cm}^{-1}$  and  $1636\text{ cm}^{-1}$  were the presence of O-H and C=O stretching, respectively [39]. The bands at around  $700\text{--}900\text{ cm}^{-1}$  were belonging to O-H out of plane bending modes. A weak band at  $2344\text{ cm}^{-1}$  was attributed to O=C=O bond group of carbonyl and the broader mode around  $3420\text{ cm}^{-1}$  is due to  $\text{H}_2\text{O}$  molecule [40]. The band at  $1432\text{ cm}^{-1}$  and  $2517\text{ cm}^{-1}$  were attributed to C-H and S-H [41]. The bands can infer that there are exist several oxygen groups such as -COOH, -OH and C=O in BC.

In addition, FTIR analysis of DM shows several main bands at  $3432$ ,  $1426$ ,  $878$  and  $714\text{ cm}^{-1}$ . The band at  $3006\text{ cm}^{-1}$  and  $2890\text{ cm}^{-1}$  in DM were brought out to be carbonate C-H asymmetrical stretching and symmetrical stretching. The strong band at  $3432\text{ cm}^{-1}$  assigned to C-O stretch of deformation of  $\text{HCO}_3^-$  group [42]. The analysis confirmed some functional groups have been transformed. Some differences spectra would indicate the bonding between the metal with active sites on the DM due to adsorption or a chemical reaction.

The XRD spectra indicated no crystal substances for BC, DM and the composite material showed in Fig. 3. The analysis of BC sample displayed a (002) peak around  $23^\circ$  and a (100) peak around  $43^\circ$ , indicating BC as an amorphous solid, similar to the bamboo-based activated carbon reported by Cheol-Soo Yang et al [39]. Thus it can be seen that the carbonate exists mainly as non-crystalline forms in BC. Unlike the DM sample which showed a classic crystal structure (Fig. 1b). The DM appear major diffraction peaks at  $29.4^\circ$  and  $30.9^\circ$ , characteristic of the (104) reflections of DM. The appearance of new crystalline phases that can be assigned to  $\text{Ca}(\text{OH})_2$  ( $18^\circ$ ,  $29.4^\circ$ ,  $33.5^\circ$  and  $50.6^\circ$ ), CaO ( $32.3^\circ$ ,  $37.4^\circ$  and  $53.4^\circ$ ), and MgO ( $42.9^\circ$  and  $64.5^\circ$ ) [39-41]. It was clearly found that peaks of DM in the XRD pattern have not altered from the analysis. There isn't any alteration in the peak position. This indicates that the crystal lattice of DM is still intact after mixing with BC.

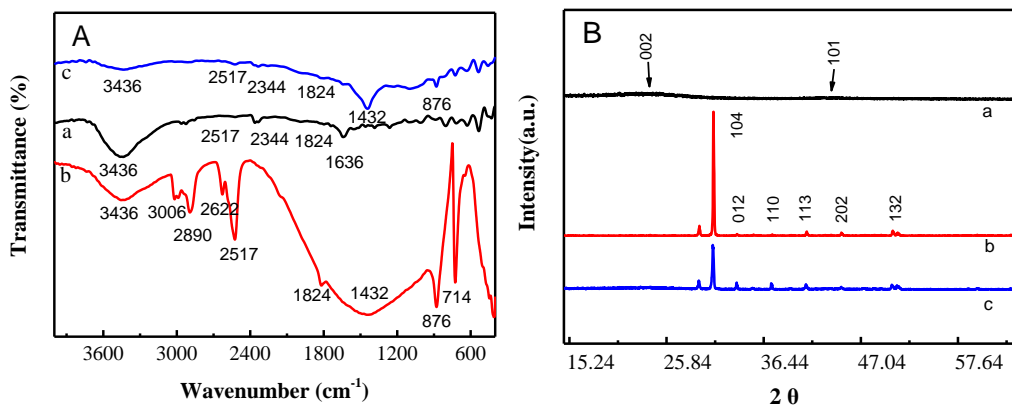


**Figure 2.** FT-IR spectra (A) and XRD analysis of three samples: (a) BC; (b) DM; and (c) BC-DM composite.

### 3.3 Electrochemical behaviors

Fig. 3 illustrated electrochemical behaviors of thiamethoxam at bare GCE (a), BC/GCE (b) and BC-DM/GCE (c) in B-R buffer (pH = 5.0), which was investigated by DPV within the potential from -0.7 to -0.3 V. Results indicated that an anodic stripping peak appeared at bare GCE (a), BC/GCE (b) and BC-DM/GCE (c), respectively. While the bare GCE showed the most weak anodic peak, and it was obviously found that the peak current of BC/GCE (b) and BC-DM/GCE (c) were much stronger than bare GCE, which is attributed the superb adsorption capacity of BC. Besides, the peak current of BC-DM/GCE (c) was stronger than that of BC/GCE (b), which indicated that in the electrochemical detection towards thiamethoxam, the BC-DM composite had better signal amplification capacity than single BC. In a word, superior electrochemical performance indicated that BC-DM composite can be an available electrode modification material for detection thiamethoxam.

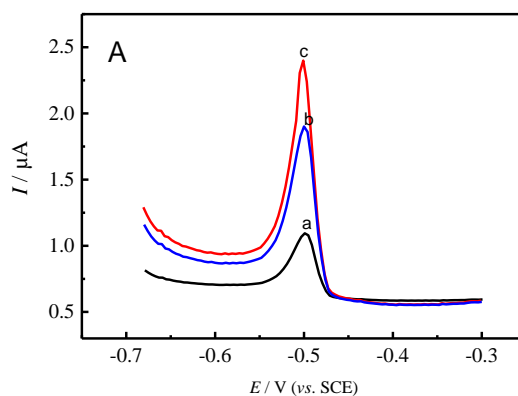


**Figure 3.** DPV responses of thiamethoxam in B-R buffer (pH = 5.0) at bare GCE (a), BC/GCE (b) and DM-BC/GCE (c).

### 3.4 Optimization of experimental conditions

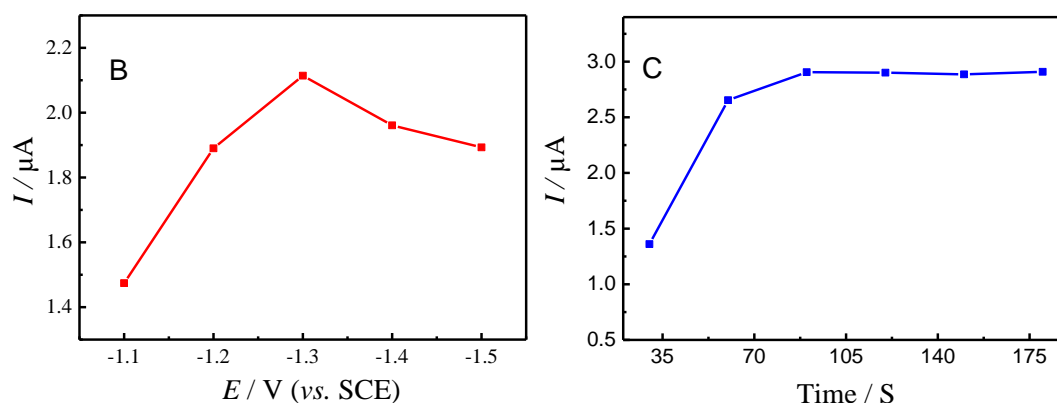
To execute the determination of thiamethoxam in real samples, key parameters towards influence of electroanalysis were optimized. DPSV was chosen to optimize the experimental parameters, including pH values of B-R solution, deposition potentials, deposition time and voltammetric measurement.

#### 3.4.1 Effect of pH

Fig. 4A illustrates the effect of pH on responses of the DM-BC/GCE in electrochemical reduction of thiamethoxam using DPV technique. It was found that the peak current increased with the change of pH from 2.0 to 5.0 and decreased with the change of pH from 5.0 to 7.0. Obviously, the maximum peak current was obtained at pH = 5.0. However, at pH = 5.0, part of DM attended the reaction and enhanced the surface area of coating modified materials. Thus, well defined of the higher peak current was obtained for the reduction of thiamethoxam at pH = 5.0. Therefore, pH = 5.0 was chosen as optimization conditions in the electrochemical detection of thiamethoxam.

#### 3.4.2 Effect of deposition potential

The absorption of thiamethoxam on the surface of DM-BC complex would increase when a voltage was applied to the working electrode. The effect of deposition potentials towards responses of thiamethoxam was studied from -1.5 to -1.1V at pH = 5.0. Fig. 4B shows the relationship between peak currents and deposition potentials, peak currents increased with the positive-shift deposition potential from -1.5 to -1.3 V, while peak currents decreased with the continuous positive-shift deposition potential from -1.3 to -1.1 V. Thus, the maximal peak current was obtained when  $E = -1.3$  V in stripping model. In following experiments, deposition potential was chosen at -1.3 V.





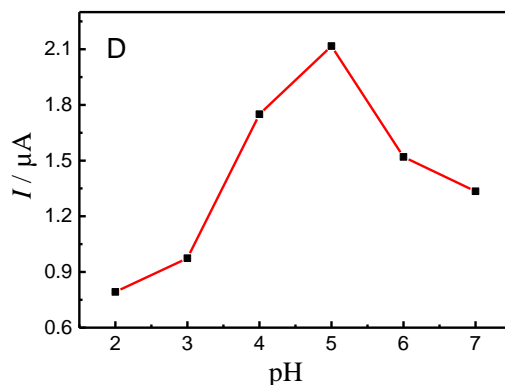


**Figure 4.** The effect of deposition potentials (B), deposition time (C), pH (D) using DPSV in B-R buffer solution containing  $15 \mu\text{g mL}^{-1}$  thiamethoxam.

### 3.4.3 Effect of deposition time

Various deposition time was measured by DPSV in 0.1 M B-R buffer solution containing of  $15 \mu\text{g mL}^{-1}$  thiamethoxam under the following conditions: pH = 5.0, deposition potential at -1.3 V. Fig. 4C shows that the peak current varies with different deposition times. As we had seen, the peak currents increased with deposition times (no more than 90 s). However, peak currents maximizing while the deposition time is greater than 90 s, which indicated that the surface of CME was saturated with the thiamethoxam when the deposition time was 90 s.

### 3.5. Linear range

Calibration plots for the determination of thiamethoxam with various concentrations on DM-BC/GCE was obtained under the optimal conditions (Fig. 5).

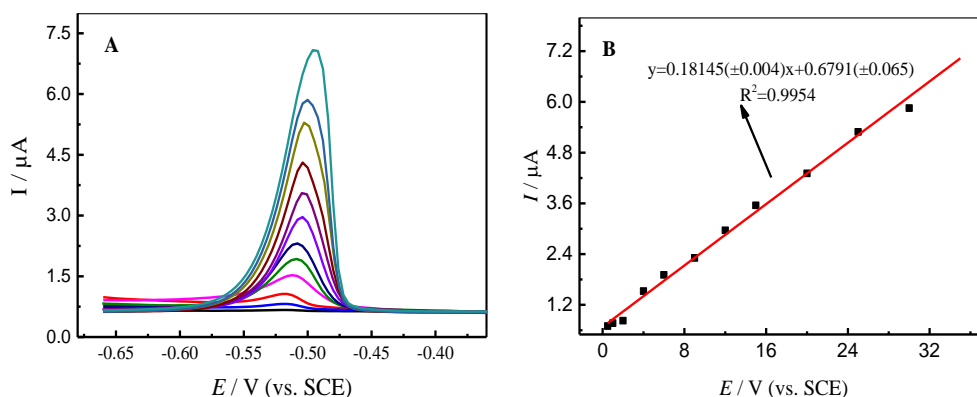


**Figure 5.** Differential pulse voltammetry responses of DM-BC/GCE in 0.1 M B-R buffer solution (pH=5.0) containing different concentrations thiamethoxam from  $0.5 - 35 \mu\text{g mL}^{-1}$  (A) and plots of DPSV peak currents vs. the corresponding thiamethoxam concentrations (B).

The DPSV was applied to investigate the oxidation process by changing the concentration of thiamethoxam in B-R buffer solution (pH = 5.0). Obviously, the oxidation peak currents increased

linearly with raising the concentrations of thiamethoxam from 0.5 to 35  $\mu\text{g mL}^{-1}$ , and the linear regression functions for thiamethoxam was  $I_{\text{pa}} = (0.1815 \pm 0.004) C + (0.6791 \pm 0.065)$  ( $R^2 = 0.9954$ ). The limits of detection (LOD) was evaluated as follows

$$\text{LOD} = 3 s/m$$

Where  $s$  is the standard deviation of the lowest concentration of the linear range, and  $m$  is the slope of linear equation. The LOD was calculated to be 0.22  $\mu\text{g mL}^{-1}$ , suggesting that the fabricated sensor possessed a better electrochemical performance for detecting thiamethoxam in a relative broad range of concentrations.

Comparison of the fabricated voltammetric sensor for the detection of thiamethoxam was listed in Table 1, obviously, DM-BC/GCE displayed better linear range and lower LOD in comparison with different electrode modified materials and voltammetric methods, suggesting that micro/nano BC displayed large surface area, good adsorption capacity and high electrocatalytic ability for the reduction of thiamethoxam, and DM synergistically enhanced electrochemical catalytic capacity of thiamethoxam, which improved sensitivity of thiamethoxam electrochemical sensor. According to literature [43], The reduction mechanism of thiamethoxam is as follow:

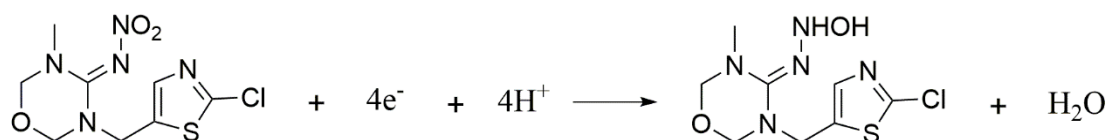


**Table 1.** The comparison of the fabricated sensor with previous reported method for the voltammetric detection of thiamethoxam.

Electrode	Method	Linear range ( $\mu\text{g mL}^{-1}$ )	Determination limit ( $\mu\text{g}$ )	Reference
BiFES/GCE	DPV	1.26 – 45.0	0.38	[1]
Hg(Ag)FE	SWV	14.9 – 78.5	0.25	[2]
m-AgSAE/GCE	DPV	Less than 14.9	0.11	[3]
GO/GCE	SWV	2.92 – 58.34	2.42	[4]
Nanosilver/SDS/GCE	DPV	0.1 – 35	0.1	[43]
MIP-GN/GC	LSW	0.5– 20	0.04	[44]
DM-BC/GCE	DPV	0.5 - 35	0.21	This work

Note: CV: cyclic voltammograms; GCE: glassy carbon electrode; DPV: differential pulse voltammograms; Gr/IL: 1-butyl-3-methylimidazolium hexafluorophosphate grapheme composite; LSV: linear sweep voltammograms.

### 3.6. Stability of modified electrode

One of the most significant factors of the CME is its reusability and stability. The stability of DM-BC/GCE for voltammetric detection of thiamethoxam was estimated by 15th successive assays (Fig. 6A). The DM-BC/GCE was renewed to remove thiamethoxam and washed by double distilled water between every test. The relative standard deviation (RSD) of replicate measurements for DM-

BC/GCE is 4.2%, suggesting that the DM-BC/GCE had a good repeatability. In addition, the CME could be used for the next detection, the current of the electrode kept an approximately invariable value with an ignorable decrease after electrode regeneration, indicating that DM-BC/GCE might be sufficient for practical applications.

### 3.7. Effects of interfering substances

Interfering substances was studied under the optimized experiment conditions to identify possible interferences, which may affect peak current signals, the selectivity of the proposed voltammetric method was investigated by addition of possible interferences at 10-fold for the effects of some metal ions and pesticide (picloram, Na<sup>+</sup>, Cu<sup>2+</sup>, K<sup>+</sup>, Fe<sup>3+</sup>, Ca<sup>2+</sup>) towards the electrochemical response of thiamethoxam have been measured. The results are displayed in Fig. 6B, it's showed most interferent substances was Cu<sup>2+</sup> with the RSD of 2.56%. In the applied potential range, interfering studies indicated unobvious decrease in the response slope. The voltammetric response shows a high selectivity for thiamethoxam in the presence of different substances.

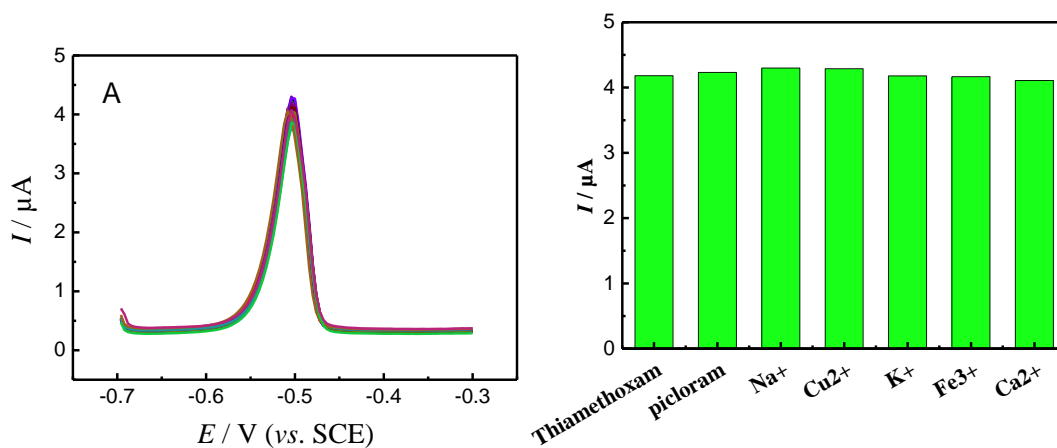


**Figure 6.** The stability of DM-BC/GCE for the DPSV detection of thiamethoxam with 15th successive assays (A) and selectivity with various metal ions and picloram.

### 3.8. Practical application

**Table 2.** Determination of thiamethoxam in all real samples using DM-BC/GCE. (n=5)

Samples	Added (μg mL <sup>-1</sup> )	Found (μg mL <sup>-1</sup> )	Recovery (%)	RSD (%)	Samples	Added (μg mL <sup>-1</sup> )	Found (μg mL <sup>-1</sup> )	Recovery (%)	RSD (%)																							
Spinach	0	< DL			River water	0	< DL																									
	6.00	6.32	105.33	0.15		15.00	15.39	102.60	0.21	25.00	23.84	95.36	0.19		0	< DL			0	< DL				6.00	6.23	103.80	0.14		6.00	6.23	103.8	0.13
	15.00	15.39	102.60	0.21		25.00	23.84	95.36	0.19		0	< DL			0	< DL				6.00	6.23	103.80	0.14		6.00	6.23	103.8	0.13				
	25.00	23.84	95.36	0.19																												
	0	< DL			0	< DL																										
	6.00	6.23	103.80	0.14		6.00	6.23	103.8	0.13																							

Rice	15.00	14.43	96.20	0.21	Farmland water	15.00	14.43	96.2	0.06
	25.00	23.89	95.56	0.11		25.00	25.89	103.56	0.18
Pear	0	< DL			Lake water	0	< DL		
	6.00	6.19	103.16	0.12		6.00	6.08	103.33	0.07
	15.00	15.33	102.20	0.17		15.00	15.13	101.07	0.12
Red soil	25.00	23.28	93.12	0.22	Tap water	25.00	24.37	97.48	0.15
	0	DL				0	DL		
	6.00	6.27	104.5	0.16		6.00	6.07	101.17	0.07
	15.00	15.33	102.2	0.22		15.00	15.17	101.13	0.12
	25.00	24.25	97.00	0.16		25.00	25.48	101.92	0.09

In order to evaluate the validity and viability of the as-prepared DM-BC nanocomposite modified electrode, this sensor for the determination of thiamethoxam was assessed by applying it to the determination of thiamethoxam in different real samples. No thiamethoxam was detected in these samples so they were spiked with appropriate amounts of thiamethoxam. The results of recovery studies were listed in Table 2. The good recoveries in all samples were in range from 93.12% to 105.33%. Clearly, the recoveries of thiamethoxam were good for all samples. These results indicated that the proposed method was feasible for the determination of thiamethoxam in different real samples.

#### 4. CONCLUSION

The sawdust from moso bamboo was collected and passed by an 1.2-mm sieve after grinding. BC was obtained by carbonizing for 2 h at 600 °C under oxygen-limited conditions and it was processed by grinding, dispersing and further processing. Water-dispersible BC was prepared by the sonication of DM assisted with BC after passing through a 74- $\mu\text{m}$  sieve. DM-BC was used as inexpensive electrode modified material for electrochemical detection of thiamethoxam in a wide liner range from 0.5 – 35  $\mu\text{g mL}^{-1}$  with the LOD of 0.22  $\mu\text{g mL}^{-1}$ . In addition, the DM-BC modified electrode exhibited well stability and satisfactory sensing response. All results revealed that thick-walled moso as biochar with post-modification provides a potential candidate for promising applications in electrochemistry.

#### ACKNOWLEDGEMENTS

The authors would like to acknowledge the financial support of this work by National Science Foundation of China (31601833), National Key R&D Program of China (2017YFD0301605), Jiangxi Outstanding Young Talents Funding Scheme (20162BCB23030), Projects of Water Science and Technology of Jiangxi Province (KT201739, 201820TG03), and Scientific Research Key Project of Jiangxi Provincial Department of Education (GJJ160351).

#### References

1. V.J. Guzsvany, F.F. Gaal, L.J. Bjelica, S.N. ÖKRÉSZ, *J. Serb. Chem. Soc.*, 70 (2005) 735.
2. R. Nauen, U. Ebbinghaus-Kintscher, V.L. Salgado, M. Kaussmann, *Pestic. Biochem. Physiol.*, 76 (2003) 55-69.
3. S.B. Singh, G.D. Foster, S.U. Khan, *J. Agric. Food Chem.*, 52 (2004) 105-109.

4. H. Obana, M. Okihashi, K. Akutsu, Y. Kitagawa, S. Hori, *J. Agric. Food Chem.*, 51 (2003) 2501-2505.
5. D. Zywitz, M. Anastassiades, E. Scherbaum, *Dtsch. Lebensm. Rundsch.*, 99 (2003) 188-196.
6. H.J. Kim, S. Liu, Y.S. Keum, Q. X. Li, *J. Agric. Food Chem.*, 51 (2003) 1823-1830.
7. A. Navalón, R. El-Khattabi, A. González-Casado, J.L. Vilchez, *Microchim. Acta*, 130 (1999) 261-265.
8. D. Zhao, J. Zhang, E. Duan, J. Wang, *Appl. Surf. Sci.*, 254 (2008) 3242-3247.
9. P. Liao, Z. Zhan, J. Dai, X. Wu, W. Zhang, K. Wang, S. Yuan, *Chem. Eng. J.*, 228 (2013) 496-505.
10. J.W. Ma, H. Wang, F.Y. Wang, Z.H. Huang, *Sep. Sci. Technol.*, 45 (2010) 2329-2336.
11. L. Zhu, Z.H. Huang, D. Wen, F. Kang, *J. Phys. Chem. Solids*, 71 (2010) 704-707.
12. Y. Wang, X. Wang, X. Wang, M. Liu, Z. Wu, L. Yang, S. Xia, J. Zhao, *J. Ind. Eng. Chem.*, 19 (2013) 353-359.
13. Y. Wang, X.J. Wang, M. Liu, X. Wang, Z. Wu, L.Z. Yang, S.Q. Xia, J.F. Zhao, *Ind. Crops Prod.*, 39 (2012) 81-88.
14. Y.X. Chen, X.D. Huang, Z.Y. Han, X. Huang, B. Hu, D.Z. Shi, W.X. Wu, *Chemosphere*, 78 (2010) 1177-1181.
15. L.S.Chan, W.H.Cheung, G. McKay, *Desalination*, 218 (2008) 304-312.
16. P. Liao, Z. Malik Ismael, W. Zhang, S. Yuan, M. Tong, K. Wang, J. Bao, *Chem. Eng. J.*, 195-196 (2012) 339-346.
17. E.L.K. Mui, W.H. Cheung, M. Valix, G. McKay, *J. Hazard. Mater.*, 177 (2010) 1001-1005.
18. H. Zhang, G. Zhu, X. Jia, Y. Ding, M. Zhang, Q. Gao, C. Hu, S. Xu, *J. Environ. Sci.*, 23 (2011) 1983-1988.
19. K. Mizuta, T. Matsumoto, Y. Hatate, K. Nishihara, T. Nakanishi, *Bioresour. Technol.*, 95 (2004) 255-257.
20. W.J. Liu, H. Jiang, H.Q. Yu, *Energy Environ. Sci.*, 12(2019). 1751-1779
21. X. Dong, L. He, Y. Liu, Y. Piao, *Electrochim. Acta*, 292 (2018) 55-62.
22. Z. Wu, F. Xu, C. Yang, X. Su, F. Guo, Q. Xu, G. Peng, Q. He, Y. Chen, *Bioresour. Technol.*, 275 (2019) 297-306.
23. F. Yang, S. Zhang, Y. Sun, Q. Du, J. Song, D.C.W. Tang, *Bioresour. Technol.*, 274 (2019) 379-385.
24. B.H. Cheng, R.J. Zeng, H. Jiang, *Bioresour. Technol.*, 246 (2017) 224-233.
25. C. Kalinke, V. Wosgrau, P.R. Oliveira, G.A. Oliveira, G. Martins, A.S. Mangrich, M.F. Bergamini, L.H. Marcolino-Junior, *Talanta*, 200 (2019) 18-525.
26. F.J. Chacón, M.L. Cayuela, A. Roig, M.A. Sánchez-Monedero, *Rev. Environ. Sci. Bio/Technol.*, 16 (2017) 695-715.
27. G. Liu, L. Li, K. Zhang, X. Wang, J. Chang, Y. Sheng, L. Bai, Y. Wen, *Int. J. Electrochem. Sci.*, 11 (2016) 1041-1054.
28. L. Li, K. Zhang, L. Chen, Z. Huang, G. Liu, M. Li, Y. Wen, *New J. Chem.*, 41(2017) 9649-9657.
29. Y. Wen, J. Chang, L. Xu, X. Liao, L. Bai, Y. Lan, M. Li, *J. Electroanal. Chem.*, 805 (2017) 159-170.
30. Z. Zhang, Y. Yao, J. Xu, Y. Wen, J. Zhang, W. Ding, *Appl. Clay Sci.*, 143 (2017) 57-66.
31. J. Chang, W. Xiao, P. Liu, X. Liao, Y. Wen, L. Bai, L. Li, M. Li, *J. Electroanal. Chem.*, 780 (2016) 103-113.
32. S. Lu, L. Bai, Y. Wen, M. Li, D. Yan, R. Zhang, K. Chen, *J. Solid State Electrochem.*, 19 (2015) 2023-2037.
33. Z.H. Jiang, *World bamboo and rattan*, Liaoning Science & Technology Press, Shenyang, Liaoning, 2002.
34. X. Gu, Y. Wang, C. Lai, J. Qiu, S. Li, Y. Hou, W. Martens, N. Mahmood, *Nano Res.*, 8 (2015) 129-139.
35. A. Benton, *Priority species of bamboo*. Springer, Cham, 2015: 31-41.
36. Y. Wen, J. Xu, D. Li, M. Liu, F. Kong, H. He, *Synthetic Met.*, 162(2012) 1308-1314.

37. Y. Wen, X. Duan, J. Xu, R. Yue, D. Li, M. Liu, L. Lu, H. He, *J. Solid State Electrochem.*, 16(2012) 3725-3738.
38. Y. Ge, M.B. Camarada, L. Xu, M. Qu, H. Liang, E. Zhao, M. Li, Y. Wen, *Microchim. Acta*, 185 (2018) 566
39. C.S. Yang, Y.S. Jang, H.K. Jeong, *Curr. Appl. Phys.*, 14 (2014) 1616-1620.
40. M. Zhang, B. Gao, Y. Yao, Y. Xue, M. Inyang, *Sci. Total Environ.*, 435-436 (2012) 567-572.
41. A.M. Dehkhoda, A.H. West, N. Ellis, *Appl. Catal., A*, 382 (2010) 197-204.
42. V. Kevorkijan, S.D. Skapin, I. Paulin, B. Šuštaršič, M. Jenko, *Mater. Tehnol.*, 44 (2010) 363-371.
43. A. Kumaravel, M. Chandrasekaran, *Sens. Actuat. B Chem.*, 174(2010)380-388.
44. T Xie, M Zhang, P Chen, H Zhao, X Yang, L Yao, H. Zhang, A. Dong, J. Wang Z. Wang., *RSC Adv.*, 7(2017)38884-38894

© 2019 The Authors. Published by ESG ([www.electrochemsci.org](http://www.electrochemsci.org)). This article is an open access article distributed under the terms and conditions of the Creative Commons Attribution license (<http://creativecommons.org/licenses/by/4.0/>).